Cavity-Ring-Down Spectroscopy on Water Vapor in the Range 555–604 nm

H. Naus,* W. Ubachs,* P. F. Levelt,† O. L. Polyansky,‡,1 N. F. Zobov,‡,1 and J. Tennyson‡

*Laser Centre, Department of Physics and Astronomy, Vrije Universiteit, Amsterdam, Netherlands; †Royal Netherlands Meteorological Institute, De Bilt, Netherlands; and ‡Department of Physics and Astronomy, University College London, Gower Street, London WC1E 6BT, United Kingdom

The method of pulsed cavity-ring-down spectroscopy was employed to record the water vapor absorption spectrum in the wavelength range 555–604 nm. The spectrum consists of 1830 lines, calibrated against the iodine standard with an accuracy of 0.01 cm^{-1}; 800 of these lines are not obtained in the HITRAN 96 database, while 243 are not included in the newly recorded Fourier transform spectrum of the Reims group. Of the set of hitherto unobserved lines, 111 could be given an assignment in terms of rovibrational quantum numbers from a comparison with first principles calculations. © 2001 Academic Press

1. INTRODUCTION

The absorption spectrum of water in the gas phase is important and complicated. Purely rotational and rovibrational absorptions within the ground electronic configuration extend from the far-infrared to the near-ultraviolet part of the spectrum with a spectral density of many lines per reciprocal centimeters. From an atmospheric physics perspective water vapor is the most important greenhouse gas absorber. The Earth's radiation budget is still not fully understood and the missing part on the absorption side might be ascribed to water vapor, either to the monomeric form or to clusters involving H_2O molecules. Our motivation for recording part of the visible absorption spectrum of H_2O is also related to an atmospheric issue: the retrieval of water vapor column densities from satellite data, such as recorded by the Global Ozone Monitoring Experiment (GOME) aboard the ERS-2 satellite. In the visible range covered by the GOME instrument (240–800 nm) there exist three spectral windows of pronounced spectral features related to water vapor, centered at 590, 650, and 720 nm. Our goal is to provide improved data for the weakest of these spectral ranges (585–600 nm) where atmospheric saturation effects play a minor role (*1*).

Also from an astrophysics perspective, water and water vapor, after H_2 and CO the third most abundant gaseous species in the universe, have recently gained interest. Observation of water vapor in sunspots (*2, 3*) has driven most of the theoretical efforts to bring the calculational methods to the level of spectroscopic accuracy (*4–9*). The water molecule, as a light triatomic true asymmetric rotor system, is a benchmark system for testing theoretical methods. Studies on H_2O have served to bring about an essential shift in the theoretical perspective from perturbative expansions of effective Hamiltonians to first principles, variational formulations of the problem, including a relativistic treatment of the electronic motion (*6*) and allowance for non-Born–Oppenheimer effects (*5*).

In the last decade the water spectrum collected in the HITRAN 96 database (*10*), which was based on a number of publications (*11–15*), has served as a reference in atmospheric modeling. In view of inconsistencies and inaccuracies (*16*), the need for improved laboratory data has become apparent. A collaboration between the Brussels/Waterloo/Reims groups (*17*) have reinvestigated the water vapor spectrum in the near-infrared, visible, and near-ultraviolet range (467–763 nm) by means of Fourier transform spectroscopy. Some groups have applied modern laser spectroscopic techniques to study the H_2O spectrum in a limited wavelength range; intracavity laser measurements (*18*) and cavity-ring-down spectroscopy (*19*) were applied. Here we present a recording of the water vapor spectrum in the range 555–604 nm, measured by pulsed cavity-ring-down spectroscopy. In this limited range 243 completely new transitions were found that did not appear in the HITRAN 96, nor in the new Fourier transform spectrum (*17*). By comparison with the calculated line lists, based on the recently developed variational methods, a number of 111 of these transitions could be assigned in terms of rovibrational quantum numbers. Additionally seven lines could be assigned to transitions in $H_2{}^{18}O$.

2. EXPERIMENTAL RESULTS

The experimental arrangement used in the present study is a typical pulsed-laser cavity-ring-down (CRD) setup that has
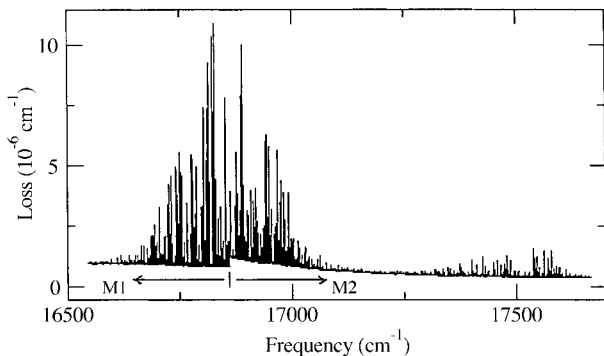
FIG. 1. H_2O overview absorption spectrum recorded in the wavelength range 555–604 nm at a pressure of 16.4 mbar and $T = 295$ K by the method of cavity-ring-down spectroscopy. The wavelength dependent background is due to the reflectivity of the mirrors; mirror sets M1 and M2 were used at the red and blue side of 16 700 cm^{-1}.

been described previously in some detail (*20, 21*). Tunable pulsed-laser radiation with a bandwidth of 0.05 cm^{-1} was obtained from a Nd:YAG pumped dye laser system (Quanta-Ray PDL-3). The ring-down cell was 85 cm long and two mirror sets with reflectivities of R ≈ 99.99% were used to cover the range 555– 604 nm. After evacuation the water vapor was leaked into the cell and the pressure was given 2 h time to stabilize. During the spectral measurements the pressure was recorded online by means of a capacitance manometer (Edwards 600 AB baratron) with an absolute accuracy of 0.15%; spectra were taken at a pressure of ≈16 mbar and a temperature of 295 K. The spectral intensities were corrected for slight variations in the molecular density during the course of the scans. Data points were taken at a stepsize of 0.01 cm^{-1} with averaging of five laser pulses per frequency position. The cavity decay constants were evaluated online from a fit to the first five characteristic times τ, as is usual in CRD spectroscopy (*22*). A plot of the deduced values of decay rates then represents the spectrum; the baseline represents the decay rate of the empty cavity, i.e., the combined reflectivity of the mirrors. An overview of the entire set of recordings is represented in Fig. 1. The vertical scale of Fig. 1 represents the loss rate of the ring-down cavity, including both the effects of mirror reflectivity and molecular absorption. The offset jump at 16 700 cm^{-1} signifies the difference in reflectivity between the two mirror sets.

Simultaneously with the recording of the water vapor spectrum, an absorption spectrum of molecular iodine was measured for wavelength calibration. In Fig. 2 such a simultaneous recording of a part of the spectrum is displayed. After converting the CRD decay transients into a water vapor absorption spectrum, the H_2O resonances were calibrated, using well-known interpolation techniques and the I_2 reference atlas (*23*). This results in an absolute accuracy for the transition frequencies of better than 0.01 cm^{-1} for each individual line. By this

means a total number of 1843 lines were clearly distinguishable from the background noise level. Of this set 13 weak lines were judged to originate from a side mode of the laser and further discarded from the data set. It should be noted that the noise-equivalent detection limit, on the order of 10^{-8}–10^{-9} cm^{-1}, is dependent on the specific reflectivity of the mirrors and hence varies over the range under study.

The entire data set of 1830 water vapor absorption lines is listed in an appendix (to be found in the electronic database of this Journal). Also listed are estimated linestrengths for the transitions. However these linestrengths should be taken as indicative only. In the case of a pulsed CRD experiment, the observed decay transients remain exponential only in the case that the bandwidth of the laser pulse is considerably smaller than the width of the absorption resonance; if this is not true the derived absorption strengths are systematically underestimated (*24*). A detailed assessment of linestrengths by means of cavity-ring-down spectroscopy will be pursued in the future. The appendix also lists the transition frequencies of the HITRAN database or the Reims experiment (*17*), whenever available. A detailed comparison based on the 1587 lines, also previously obtained, reveals that the average deviation between the two data sets is -0.004 ± 0.004 cm^{-1}, with a 1σ uncertainty.

3. LINE ASSIGNMENTS

Line assignments were performed using techniques developed to analyze other short wavelength water spectra (*17, 25*). This technique relies on comparisons with linelists of water transitions calculated using variational techniques. In the present work the analysis was performed with linelists computed using a spectroscopically determined potential energy surface and completely ab initio procedures (*5, 25*). As has been discussed elsewhere (*25*), these linelists provide complementary information. However, it should be noted that the frequencies analyzed here are near the limits of reliability of Partridge and Schwenke's spectroscopically determined poten-
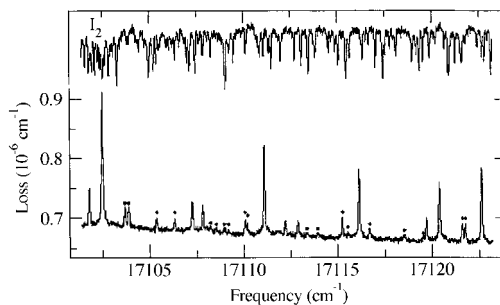
FIG. 2. Recording of a detail spectrum in the range 17 100–17 122 cm^{-1} of relatively weak resonances; the upper spectrum is an online recording of the I_2-absorption spectrum used for wavelength calibration. The lines marked with a dot are not contained in the HITRAN database.

TABLE 1
Newly Observed and Assigned Water Vapor Lines in the Range 555–604 nm

Frequency	J'Ka'Kc'			J"Ka"Kc"			v'	comment	Frequency	J'Ka'Kc'			J"Ka"Kc"			v'	comment
16692.054	6	1	6	6	1	5	321	nn	17137.638	8	4	5	7	3	4	420	nn
16706.331	8	6	3	8	6	2	401	nn	17153.243	4	3	2	3	3	1	043	nn
16707.782	6	3	4	7	1	7	241	nn	17164.023	3	1	3	3	3	0	123	nc
16710.320	1	1	1	2	2	0	142	nn	17170.484	5	5	1	5	5	0	043	nn
16722.708	7	6	1	7	6	2	401	nn	17176.666	8	3	5	7	2	6	420	nn
16731.137	8	5	3	8	5	4	401	nn	17183.690	7	5	2	8	5	3	203	nn
16762.938	4	3	2	4	1	3	241	nn	17189.735	8	4	5	7	1	6	500	nn
16779.478	3	2	2	3	3	1	142	nn	17190.909	6	5	1	5	4	2	420	nn
16781.742	5	1	5	5	2	4	500	nn	17197.182	4	3	2	5	3	3	123	nn
16790.505	6	3	3	5	3	2	241	nc	17207.299	6	5	1	6	6	0	302	nc
16808.955	5	3	3	5	4	2	142	nn	17221.505	7	2	6	8	1	7	302	nn
16823.485	2	2	1	2	2	0	321	nn	17242.404	4	2	2	5	3	3	302	nc
16836.923	8	4	4	7	5	3	500	nn	17246.503	6	1	5	7	2	6	302	nn
16842.177	5	4	2	4	4	1	241	nn	17271.415	3	1	3	4	2	2	302	nc
16846.013	6	2	4	5	1	5	340	nn	17272.780	4	1	3	4	0	4	222	nn
16852.026	6	3	3	6	1	6	241	nn	17282.102	9	2	8	9	2	7	203	nn
16863.662	5	3	3	5	3	2	321	nn	17283.153	6	3	4	6	4	3	302	nn
16876.272	2	1	2	2	1	1	401	nn	17284.521	5	1	5	5	3	2	203	nn
16887.282	6	5	1	6	4	2	500	nn	17288.544	4	1	3	3	2	2	222	nn
16891.468	4	1	3	3	2	2	142	nn	17291.992	2	2	1	2	1	2	222	nc
16898.751	5	5	1	5	4	2	500	nc	17292.136	3	1	3	2	0	2	222	nn
16900.443	8	4	4	7	4	3	241	nn	17296.439	8	1	7	8	3	6	203	nn
16911.802	9	2	8	9	1	9	500	nn	17302.437	4	3	1	5	1	4	123	nc
16912.225	8	2	7	8	0	8	321	nn	17305.753	3	0	3	4	2	2	203	nn
16915.142	7	5	3	6	5	2	401	nn	17322.300	7	0	7	6	1	6	222	nn
16917.548	5	5	1	5	5	0	241	nn	17362.560	4	2	2	4	3	1	302	nn
16933.586	9	5	5	8	5	4	401	nn	17367.241	6	2	5	5	1	4	222	nn
16947.563	10	2	8	9	1	8	420	nn	17398.949	3	3	1	2	2	0	222	nn
16960.802	7	2	6	7	1	7	142	nn	17401.893	4	2	2	3	1	3	222	nc
16966.545	9	2	7	8	3	6	500	nn	17402.203	6	3	4	7	4	3	104	nc
16969.152	9	3	6	8	4	5	500	nn	17431.226	6	3	4	5	2	3	222	nn
16973.240	1	1	1	1	1	0	043	nn	17447.988	6	6	1	6	5	2	302	nn
16974.785	8	4	5	7	3	4	340	nn	17471.944	6	2	4	6	1	5	302	nn
16977.143	10	2	8	9	2	7	401	nn	17487.863	5	4	1	4	3	2	222	nc
16985.090	9	2	7	8	2	6	401	nn	17501.383	8	5	4	7	5	3	203	nn
16989.330	7	0	7	6	1	6	500	nn	17502.183	8	5	3	7	5	2	203	nn
16994.280	8	3	6	7	2	5	500	nn	17509.585	4	2	3	5	3	2	104	nn
16996.102	2	1	1	2	1	2	043	nn	17510.858	6	2	4	5	3	3	302	nn
17003.441	7	3	5	6	0	6	340	nn	17517.943	7	2	6	7	1	7	302	nn
17009.339	7	1	6	6	1	5	401	nn	17534.105	5	5	1	4	4	0	222	nn
17021.680	6	4	3	5	4	2	321	nn	17541.145	3	2	2	3	0	3	203	nc
17025.000	9	1	8	8	2	7	142	nn	17546.251	3	2	2	2	1	1	302	nn
17026.585	4	2	2	3	1	3	142	nn	17580.380	2	2	0	3	3	1	104	nn
17035.195	3	1	3	2	1	2	043	nn	17581.469	8	5	3	7	4	4	302	nn
17039.610	7	7	0	6	6	1	500	nn	17600.082	5	1	5	6	0	6	104	nn
17045.013	8	7	2	7	6	1	500	nn	17604.353	6	1	6	6	2	5	104	nc
17052.726	8	5	4	7	4	3	500	nn	17609.096	6	4	3	5	1	4	222	nn
17063.164	8	3	6	7	2	5	420	nn	17609.449	4	3	1	4	1	4	203	nn
17070.876	6	2	4	5	1	5	420	nn	17618.883	9	2	7	8	2	6	203	nn
17075.750	6	1	6	5	1	5	043	nn	17625.389	4	0	4	5	1	5	104	nn
17085.313	5	1	5	6	0	6	222	nn	17628.687	2	1	1	3	2	2	104	nn
17117.694	6	2	5	6	3	4	222	nn	17628.961	5	1	4	4	4	1	104	nc
17122.098	6	4	3	5	3	2	420	nn	17632.410	5	4	2	4	2	3	123	nn
17125.776	6	2	4	7	2	5	123	nn	17658.343	6	6	1	5	5	0	222	nn
17136.913	5	3	2	5	4	1	222	nn	17665.018	8	5	4	7	4	3	302	nn
17137.497	6	2	5	7	2	6	123	nn									

nc assignment made on basis of combination difference
nn assignment made on basis of single transition

tial and, in particular, the vibrational labels given by this linelist were generally not correct.

Linelists, combined where appropriate with an allowance for systematic errors associated with a particular vibrational band, were used to identify candidate line assignments based on both frequency and intensity considerations. These assignments

TABLE 2
Assigned $H_2^{18}O$ Lines in the Range 555–604 nm

Frequency	Intensity	Previous	J'	Ka'	Kc'	J"	Ka"	Kc"	v'–v"
16761.672	3.57E-27	16761.6749	3	1	3	4	1	4	401–000
16769.400	7.14E-27	16769.3977	4	4	0	4	4	1	401–000
16769.400	7.14E-27	16769.3977	2	1	1	3	1	2	401–000
16780.344	7.14E-27		2	2	0	2	2	1	321–000
16783.584	1.07E-26	16783.5735	2	0	2	3	0	3	401–000
16843.473	9.88E-27	16843.4709	2	2	0	2	2	1	401–000
16845.943	6.42E-27	16845.9774	4	0	4	3	0	3	321–000

were then used to predict other lines using combination differences; the presence of these predicted lines allows a further assignment to be made as well as confirming the original assignment. In some cases it is not possible to use combination differences to confirm line assignments. This does not invalidate the original assignment if the predicted line lies outside the frequency range of the spectrum, or under another stronger line, or is too weak to be observed.

The 1830 observed lines can be distinguished in several subsets. About a thousand were already contained in the HITRAN database, whereas nearly 1600 were observed in the recent Fourier transform spectrum (17). Two hundred forty-three lines were not previously observed in either the HITRAN or the Reims spectra. Table 1 presents a subset of the 111 newly observed transitions that have been positively assigned to $H_2^{16}O$ transitions belonging to the 5ν polyad. All transitions originate in the (0, 0, 0) ground vibrational level. The table distinguishes between assignments which have been confirmed by combination differences, which can be regarded as secure, and those for which only a single transition involving the upper energy level has been observed, for which occasional misassignments are possible. The extra information available in the new spectrum and our new ab initio linelist (25), which is much more reliable for states with high K_a, means that further assignments are possible. One hundred ninety-six previously unassigned lines seen both here and in the earlier spectrum of Carleer et al. (17) have been assigned; hence the analysis of the present data have aided in the assignment of previously obtained sets of data. These assignments are included in the archived table.

Besides the $H_2^{16}O$ lines discussed above, we have been able assign seven of the newly observed lines to transitions of $H_2^{18}O$. These lines, listed in Table 2, belong to the (401) and (321) vibrational transitions and are the first $H_2^{18}O$ lines, which have been assigned to the 5ν polyad. The 5ν polyad is already weak for $H_2^{16}O$ transitions and $H_2^{18}O$ is only present in natural abundance of 0.02% in the spectrum. The observation of these $H_2^{18}O$ transitions are an additional illustration of the sensitivity of the cavity-ring-down technique.

Observation of new short wavelength transitions of $H_2^{16}O$ yields new information about the energy levels of this important molecule. The data reported in this paper will be included in a comprehensive new compilation of water energy levels (26).

REFERENCES

1. A. N. Maurellis, R. Lang, W. van der Zande, I. Aben, and W. Ubachs, *Geophys. Res. Lett.* **27,** 903–906 (2000).
2. L. Wallace, P. F. Bernath, W. Livingston, K. Hinkle, J. Busler, B. Guo, and K. Zhang, *Science* **268,** 1155–1158 (1995).
3. O. L. Polyansky, N. F. Zobov, S. Viti, J. Tennyson, P. F. Bernath, and L. Wallace, *Science* **277,** 346–348 (1997).
4. O. L. Polyansky, N. F. Zobov, S. Viti, and J. Tennyson, *J. Mol. Spectrosc.* **189,** 291–300 (1998).
5. O. L. Polyansky, J. Tennyson, and N. F. Zobov, *Spectrochim. Acta Part A* **55,** 659–693 (1999).
6. A. G. Császár, J. S. Kain, O. L. Polyansky, N. F. Zobov, and J. Tennyson, *Chem. Phys. Lett.* **293,** 317–323 (1998); *Chem. Phys. Lett.* **312,** 613–616 (1999).
7. J. S. Kain, O. L. Polyansky, and J. Tennyson, *Chem. Phys. Lett.* **317,** 365–371 (2000).
8. H. Y. Mussa and J. Tennyson, *J. Chem. Phys.* **109,** 10885–10892 (1998).
9. H. Partridge and D. W. Schwenke, *J. Chem. Phys.* **106,** 4618–4639 (1997).
10. L. S. Rothman, C. P. Rinsland, A. Goldman, S. T. Massie, D. P. Edwards, J. M. Flaud, A. Perrin, C. Camy-Peret, V. Dana, J.-Y. Mandin, J. Schroeder, A. McCann, R. R. Gamache, R. B. Watson, K. Yoshino, K. V. Chance, K. W. Jucks, L. R. Brown, V. Nemtchinov, and P. Varanasi, *J. Quant. Spectrosc. Radiat. Transfer* **60,** 665–710 (1998).
11. C. Camy-Peyret, J.-M. Flaud, J.-Y. Mandin, J. P. Chevillard, J. Brault, D. A. Ramsay, M. Vervloet, and J. Chauville, *J. Mol. Spectrosc.* **113,** 208–228 (1985).
12. J.-Y. Mandin, J. P. Chevillard, C. Camy-Peyret, J.-M. Flaud, and J. W. Brault, *J. Mol. Spectrosc.* **116,** 167–190 (1986).
13. J.-Y. Mandin, J. P. Chevillard, J.-M. Flaud, and C. Camy-Peyret, *Can. J. Phys.* **66,** 997–1011 (1988).

14. J. P. Chevillard, J.-Y. Mandin, J.-M. Flaud, and C. Camy-Peyret, *Can. J. Phys.* **67,** 1065–1084 (1989).
15. R. A. Toth, *J. Mol. Spectrosc.* **166,** 176–183 (1994).
16. L. P. Giver, C. Chackerian, and P. Varanasi, *J. Quant. Spectrosc. Radiat. Transfer* **66,** 101–105 (2000).
17. M. Carleer, A. Jenouvrier, A.-C. Vandaele, P. F. Bernath, M. F. Mérienne, R. Colin, N. F. Zobov, O. L. Polyansky, J. Tennyson, and V. A. Savin, *J. Chem. Phys.* **111,** 2444–2450 (1999).
18. B. Kalmar and J. J. O'Brien, *J. Mol. Spectrosc.* **192,** 386–393 (1998).
19. J. Xie, B. A. Paldus, E. H. Wahl, J. Martin, T. G. Owano, C. H. Kruger, J. S. Harris, and R. N. Zare, *Chem. Phys. Lett.* **284,** 387–395 (1998).
20. H. Naus, A. de Lange, and W. Ubachs, *Phys. Rev. A: Gen. Phys.* **56,** 4655–4763 (1997).
21. H. Naus and W. Ubachs, *Appl. Opt.* **38,** 3423–3428 (1999).
22. M. D. Wheeler, S. N. Newman, A. J. Orr-Ewing, and M. Ashfold, *J. Chem. Soc., Faraday Trans.* **94,** 337–352 (1998).
23. S. Gerstenkorn and P. Luc, Atlas du Spectroscopie d'Absorption de la Molécule de l'Iode Entre 14800–20000 cm^{-1}, Presses du CNRS, Paris, 1978.
24. P. Zalicki and R. N. Zare, *J. Chem. Phys.* **102,** 2708–2717 (1995).
25. N. F. Zobov, D. Belmiloud, O. L. Polyansky, J. Tennyson, S. V. Shirin, M. Carleer, A. Jenouvrier, A.-C. Vandaele, P. F. Bernath, M. F. Mérienne, and R. Colin, *J. Chem. Phys.* **113,** 1546–1552 (2000).
26. J. Tennyson, N. F. Zobov, R. Williamson, O. L. Polyansky, and P. F. Bernath, unpublished manuscript.